Journal of Power Sources 195 (2010) 720–728

Contents lists available at ScienceDirect

Journal of Power Sources

journal homepage: www.elsevier.com/locate/jpowsour

Dopants to enhance SOFC cathodes based on Sr-doped $LaFeO_3$ and $LaMnO_3$

F. Bidrawn[a], G. Kim[a,b], N. Aramrueang[a], J.M. Vohs[a], R.J. Gorte[a,*]

[a] Department of Chemical and Biomolecular Engineering, University of Pennsylvania, 311 Towne Building, 220 South 33rd Street, Philadelphia, PA 19104, USA
[b] School of Energy Engineering, Ulsan National Institute of Science and Technology (UNIST), San 194, Banyeon-ri, Eonyang-eup, Ulsan 689-805, Republic of Korea

ARTICLE INFO

Article history:
Received 14 July 2009
Received in revised form 11 August 2009
Accepted 13 August 2009
Available online 20 August 2009

Keywords:
Solid oxide fuel cells
Cathodes
Yttria-stabilized zirconia
Lanthanum ferrate
Lanthanum manganate
Dopants

ABSTRACT

The influence of various infiltrated dopants on the performance of solid oxide fuel cell (SOFC) cathodes was examined. The cathodes were prepared by infiltration of nitrate salts into porous yttria-stabilized zirconia (YSZ) to produce composites with 40-wt% of either $La_{0.8}Sr_{0.2}FeO_3$ (LSF) or $La_{0.8}Sr_{0.2}MnO_3$ (LSM) and were then calcined to either 1123 or 1373 K. The addition of dopants had little influence on the 1123-K composite electrodes but all dopants tested improved the performance of the 1373-K composites. With 1373-K, LSF–YSZ electrodes, the open-circuit impedances decreased dramatically following the addition of 10-wt% YSZ, 0.5-wt% Pd, 10-wt% $Ce_{0.8}Sm_{0.2}O_{1.9}$ (SDC), 10-wt% CaO, and 10-wt% K_2O. Similarly, the 1373-K, LSM–YSZ electrodes were enhanced by the addition of 10-wt% CeO_2, 1-wt% Pd, and 10-wt% YSZ. Since the improved performance was close to that of the corresponding LSF–YSZ and LSM–YSZ electrodes that had been calcined to only 1123 K, it is suggested that the improved performance is related to structural changes in the electrode, rather than to improved catalytic properties or ionic conductivity.

1. Introduction

The performance-limiting factor in state-of-the-art solid oxide fuel cells (SOFC) is often the cathode impedance [1–3]. Despite the fact that composites of Sr-doped $LaMnO_3$ (LSM) and YSZ exhibit relatively high impedances at temperatures below 1023 K, these composites are still the standard materials in SOFC cathodes that utilize YSZ electrolytes because of their long-term stabilities [4]. Electrodes based on alternative, mixed-conducting perovskites either undergo solid-state reactions with YSZ at the sintering temperatures required for standard preparation of SOFC electrodes [2,5] or otherwise interact with the YSZ in such a way as to decrease cathode performance [6].

There has been a considerable effort aimed at improving the performance of LSM–YSZ composites by adding catalytic or ion-conducting components to the composite electrode after it has been formed. The primary idea behind adding catalytic components is presumably to increase the rate of O_2 dissociation, while the addition of ionic or mixed-conducting materials should widen the three-phase boundary (TPB). Although there is still no consensus on what is the rate-limiting step that determines the impedance of LSM–YSZ cathodes, there are some intriguing observations that suggest that one can indeed enhance their performance by infiltration of a "promoter", as discussed in the next paragraphs.

For example, the addition of catalytic components has met with mixed success. While Uchida et al. found that the addition of Pt significantly enhanced the electrochemical performance of LSM–YSZ composites [7] and Erning et al. reported similar enhancements through the addition of Pd [8], Haanappel et al. reported that neither Pd nor Pt had any effect on the performance of LSM cathodes [9]. Discrepancies also exist for claims about the effect of infiltrated cobalt oxide. Yamahara et al. reported significant improvements in cathode performance following the addition of small Co_3O_4 nanoparticles [10,11]; Huang et al. [12] claimed that the incorporation of CoO_x had no effect on LSM–YSZ cathode impedances.

There does seem to be agreement that the addition of mixed-conducting perovskites, either Sr-doped $LaCoO_3$ [13], Sr-doped $SmCoO_3$ [14], or Sr-doped $LaFe_{0.8}Co_{0.2}O_3$ [15], can decrease cathode overpotentials. While the reactivity of these perovskites with YSZ may preclude their being used in this application, the observation that the addition of relatively small amounts of these mixed-conducting perovskites can improve performance may indicate that they deposit preferentially at TPB sites in the LSM–YSZ composite and increase the width of those sites. Mixed conductivity at the TPB sites may also explain the improved performance of LSM–YSZ electrodes following the addition of Gd-doped ceria [16] or BiO_x [17].

Catalysis and mixed conductivity do not explain electrode promotion with all additives. For example, one study reported that infiltration of Sr salts can improve LSM cathodes [18]. SrO is unlikely to be a catalyst for O_2 dissociation and the addition of SrO is not expected to significantly change either the electronic or ionic conductivity of LSM. Indeed, the segregation of Sr to the electrolyte

* Corresponding author. Tel.: +1 215 898 4439; fax: +1 215 573 2093.
E-mail address: gorte@seas.upenn.edu (R.J. Gorte).

0378-7753/$ – see front matter © 2009 Elsevier B.V. All rights reserved.
doi:10.1016/j.jpowsour.2009.08.034

interface is often thought to cause electrode deactivation [19]. Similarly, Mogensen et al. found that adding either pure or doped ceria had a similar effect on cathode performance, even though the ionic conductivity of pure ceria should be much lower [20]. This group suggested that the improvement in LSM–YSZ electrode performance following the addition of nanoparticles might be due to gettering of impurities at the TPB sites.

A major complication in assessing how promoters change electrochemical properties is that electrode structure appears to play a very large role, not only in affecting performance, but also in determining whether or not additives will promote performance. For example, one study of $La_{0.8}Sr_{0.2}Cr_{0.5}Mn_{0.5}O_3$ (LSCM) anodes fabricated by traditional ceramics-processing methods found that the addition of Pd had minimal effect on performance in H_2 [21], whereas studies of electrodes formed by infiltration of LSCM into porous YSZ demonstrated that the addition of even 0.5-wt% Pd increased the power density of cells by a factor of five [22]. Since the structure of LSCM–YSZ composites formed by conventional co-sintering of mixed powders is very different from that of composites formed by infiltration [23], we suggest that structural differences in the electrodes explain the apparent discrepancy.

Since variations in electrode structures may account for the differences that have been reported in the literature, regarding whether or not particular additives improve electrode performance, it seemed important to re-examine the issue of electrode promotion using a range of materials that have different properties with electrodes that have a common structure. In the present study, we investigated the effect of additives on cathode composites formed from YSZ and either LSM or $La_{0.8}Sr_{0.2}FeO_3$ (LSF). The LSM–YSZ and LSF–YSZ composite electrodes used here were prepared by infiltration of the corresponding nitrate salts into porous YSZ, so that all electrodes had a similar structure. Because previous work showed that the electrochemical properties of LSF–YSZ and LSM–YSZ composites formed by infiltration are a strong function of calcination temperature [6,24], the effect of the promoters was examined on composites that were calcined to either 1123 or 1373 K.

The specific additives that were incorporated into the LSF–YSZ and LSM–YSZ electrodes were Pd, CeO_2 (or $Ce_{0.8}Sm_{0.2}O_{1.9}$, SDC) YSZ, CaO, and K_2O. These materials were chosen for their expected function (or lack thereof). Ceria is a good oxidation catalyst [25] and could provide both ionic and electronic conductivity, particularly if it is partially reduced at TPB sites. Pd is expected to be an outstanding oxidation catalyst but should have minimal effect on either ionic or electronic conductivity in the amounts incorporated in this study, 0.5 wt%. YSZ is an outstanding ionic conductor but should provide minimal electronic conductivity or catalytic activity over that of the composite electrode itself. CaO should have minimal effect on catalytic, electronic, or ionic-conduction properties. In the case of LSF, substitution of Ca for Sr in the perovskite lattices could reduce the ionic conductivity and therefore harm performance [26]. If anything, K_2O would be expected to hurt electrode performance. Finally, since the infiltration process itself could affect electrode structure, experiments were performed with both 0.1N HNO_3 and NH_4OH solutions to test the effect that acidic and basic solutions might have on selective electrode dissolution.

A major conclusion of the present study is that electrode promotion through the addition of catalytic and conducting components is associated with electrode structure, at least for the systems studied here.

2. Experimental

The fuel cells used in this study were all prepared in a similar manner. First, a YSZ wafer, consisting of a dense layer between two porous layers, was fabricated. The porous-dense-porous YSZ structure was produced by laminating three green tapes, using graphite as the pore former in the layers that were to be porous, and then firing the structure to 1773 K for 4 h [27,28]. The green tapes were prepared by mixing YSZ powder (Tosoh Corp., 8 mol% Y_2O_3-doped ZrO_2, 0.2 μm) with distilled water, a dispersant (Duramax 3005, Rohm & Haas), and binders (HA12 and B1000, Rohm & Haas). In the present study, the dense electrolyte layers were approximately 100 μm thick for the series of cells made with LSF and 70 μm thick for the series made with LSM. For each cell, the dense electrolyte was circular, with a diameter of 1 cm, while the two porous layers were between 45 and 55 μm in thickness and 0.67 cm in diameter. The porous layers were estimated to have a porosity of 65%, with a BET surface area of ~0.3 $m^2\,g^{-1}$ [26].

To prepare the composite cathodes, the porous YSZ backbone was impregnated with aqueous solutions of $La(NO_3)_3$, $Fe(NO_3)_3$, $Mn(NO_3)_2$, and $Sr(NO_3)_2$, in the proper molar ratios. For LSF–YSZ composites, the La:Sr:Fe ratio was 0.8:0.2:1; for LSM–YSZ, the La:Sr:Mn ratio was 0.8:0.2:1. For fabrication of LSF–YSZ electrodes, citric acid was added to the solutions so that the perovskite phase could be formed at lower temperatures; but this was not necessary for the LSM–YSZ electrodes [29,30]. Multiple impregnation steps were required, and the samples were calcined to 723 K between each impregnation step until the desired 40-wt% loading of perovskite was achieved. Cells were then calcined to either 1123 or 1373 K. After calcination to form the perovskites, the precursor solution of one of the promoters was impregnated into the electrode and the sample was again calcined to either 973 or 1373 K.

For most of the cells, the anodes were added, *after* the cathodes were prepared, by impregnating 50-wt% ceria and 0.5-wt% Pd into the porous layer opposite the cathode using the nitrate salts and calcination to 723 K [31]. Silver leads were then attached

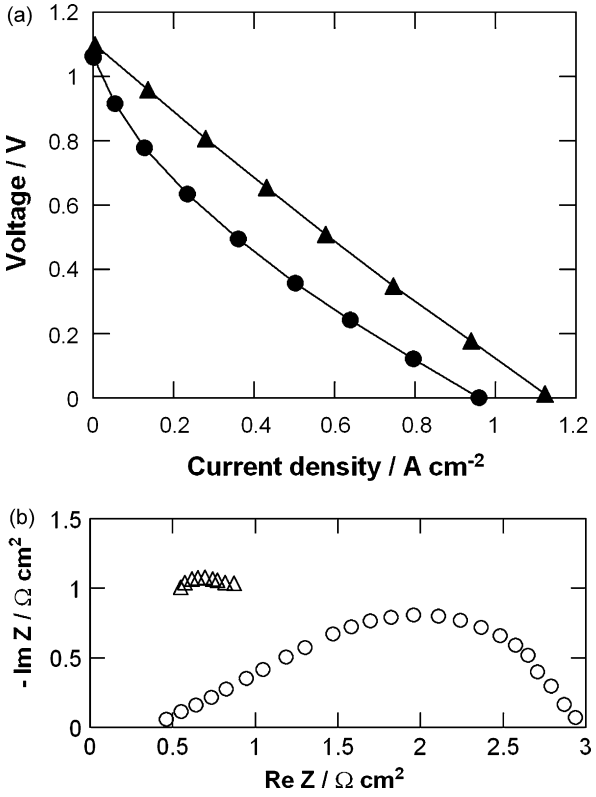

Fig. 1. (a) *V–i* polarization plots, measured at 973 K, for cells with LSF–YSZ electrodes calcined to 1123 K (▲) and 1373 K (●). (b) OCV impedance data for cells, at 973 K, with LSF–YSZ electrodes calcined to 1123 K (△) and 1373 K (◯). The spectrum for the 1123-K electrode has been offset for clarity.

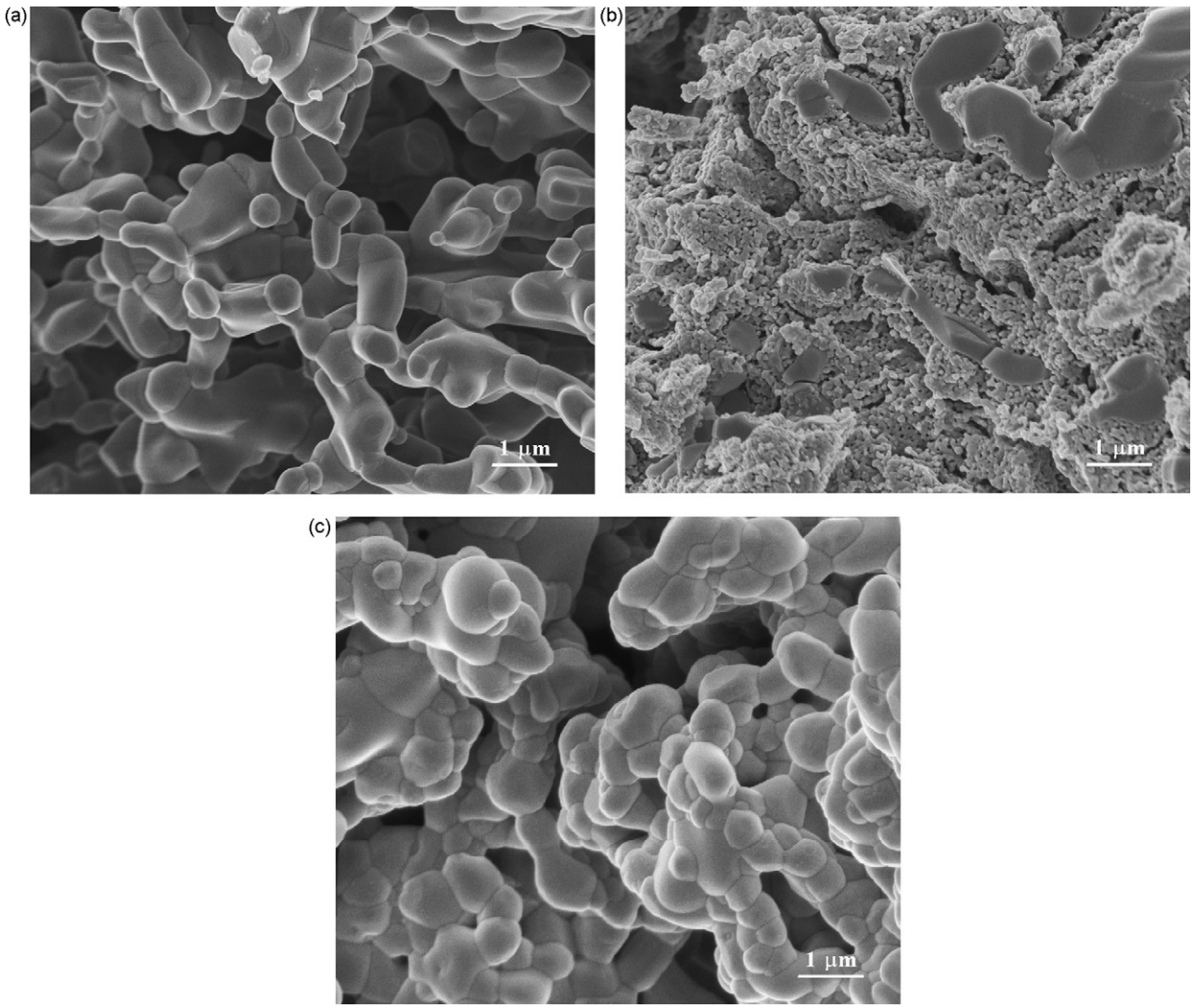

Fig. 2. (a) An SEM image of the YSZ scaffold used in electrode fabrication. (b) An SEM image of the LSF–YSZ composite prepared by calcination at 1123 K. (c) An SEM image of the LSF–YSZ composite prepared by calcination at 1373 K.

to both electrodes using silver paste. On a few cells, the anodes were based on 40-wt% LSCM ($La_{0.8}Sr_{0.2}Cr_{0.5}Mn_{0.5}O_3$) with 5-wt% ceria and 0.5-wt% Pd, prepared as described elsewhere [23]. The performance characteristics of the LSCM-based anodes were essentially indistinguishable from those of anodes made with 50-wt% ceria. Although preparation of LSCM required higher temperatures, the ceria and Pd were again added *after* the cathodes were calcined to their final temperature. The impedance of both types of anodes is reported to be between 0.1 and 0.2 $\Omega\,cm^2$ [23,31], independent of current density, when operated at 973 K in humidified (3% H_2O) H_2.

After the cells were prepared, they were mounted onto alumina tubes using a ceramic adhesive (Aremco Ceramabond 522). All cell testing was performed with the anode exposed to humidified H_2 and the cathode held in atmospheric air. Impedance spectra and *V–i* polarization curves were measured using a Gamry Instruments potentiostat. Impedance spectra were measured galvanostatically at various currents in the frequency range of 300 kHz to 0.1 Hz, with a 1-mA AC perturbation. Physical characterization of the LSM–YSZ and LSF–YSZ composites was carried out using XRD and scanning electron microscopy (SEM), with results from the unpromoted electrodes having been reported previously [24,26].

3. Results

3.1. Unpromoted LSF–YSZ and LSM–YSZ electrodes

While the characteristics of LSF–YSZ and LSM–YSZ electrodes formed by infiltration have been discussed elsewhere [24,29], the results were reproduced for the present study so that the performance of electrodes with additives could be compared for the same YSZ scaffold structure. Fuel cell data for cells made with LSF–YSZ cathodes, calcined to either 1123 or 1373 K, are shown in Fig. 1.

The *V–i* polarization curves in Fig. 1a, obtained at 973 K with humidified H_2 as the fuel, show only slight curvature for the cell with the LSF–YSZ composite cathode calcined at 1123 K but significantly more curvature for the cell with the cathode calcined at 1373 K. This effect of calcination temperature is shown more dramatically by the open-circuit voltage (OCV) Cole–Cole plots in Fig. 1b. The ohmic impedance, determined from the high-frequency intercept in the Cole–Cole plot, was ~0.5 $\Omega\,cm^2$ for both cells. This value is very close to the resistance expected for a 100-μm YSZ electrolyte [32]. The effect of increased calcination temperature was to increase the non-ohmic impedances, which are due to electrode losses and are calculated from the arc length in the Cole–Cole plots. The non-ohmic impedances at OCV were approxi-

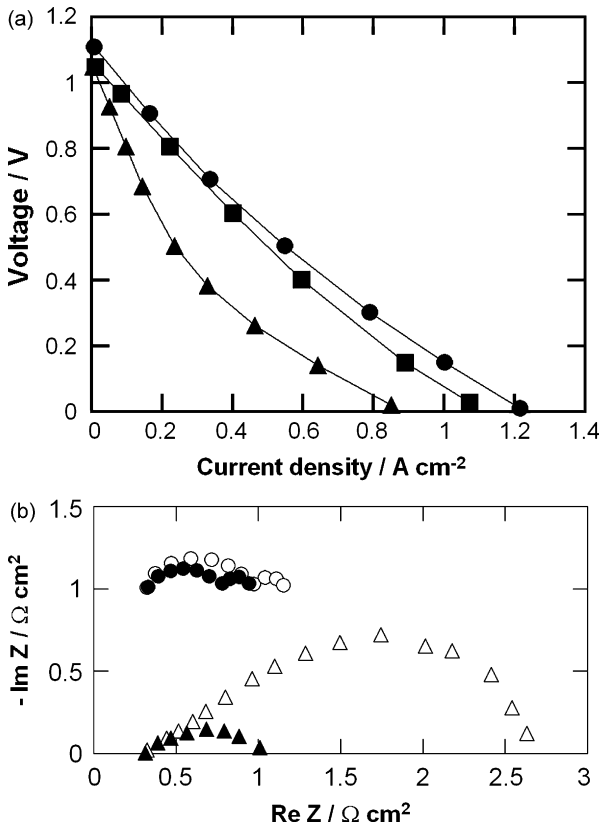

Fig. 3. (a) *V–i* polarization plots, measured at 973 K, for cells with LSM–YSZ electrodes. Data are shown for composites calcined to 1123 K (●) and 1373 K (▲), starting from open-circuit. Data are also shown for the cell with the composite calcined to 1373 K, after it had been shorted for 2 h (■). (b) OCV impedance of cells with LSM–YSZ cathodes calcined to 1123 (○) and 1373 K (△), before (open symbols) and after (closed symbols) polarization by shorting the cells for 2 h. The data were obtained at 973 K and the spectra for the 1123-K composites have been offset for clarity.

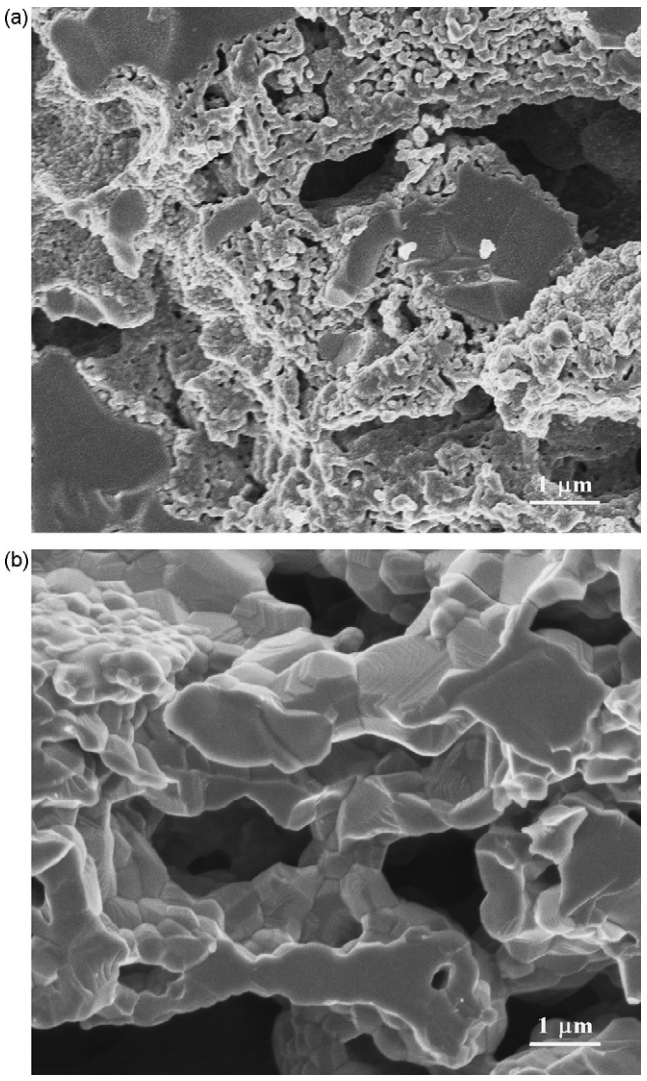

Fig. 4. (a) An SEM image of the LSM–YSZ composite prepared by calcination at 1123 K. (b) An SEM image of the LSM–YSZ composite prepared by calcination at 1373 K.

mately 0.35 Ω cm^2 for the cell with the cathode calcined to 1123 K and 2.6 Ω cm^2 for the cell with the cathode calcined at 1373 K. Assuming an anode impedance of 0.15 Ω cm^2 as determined in previous studies [23,31], most of the non-ohmic cell losses are associated with the cathodes. For the 1123-K, LSF–YSZ composite, the impedance is approximately 0.2 Ω cm^2 and independent of current density. This is slightly higher than the impedance reported previously, 0.15 Ω cm^2, possibly because the YSZ scaffold in the present study had a lower surface area [33]. For the 1373-K, LSF–YSZ composite, the impedance is approximately 2.4 Ω cm^2 at OCV. Since the slope of the *V–i* polarization curve in Fig. 1a decreases with increasing current density, the cathode impedance must decrease with current density. The OCV impedance and current dependence for the cell calcined at 1373 K are essentially identical to what was reported in a previous study [6].

The changes in the LSF–YSZ composite caused by the higher calcination temperature do not appear to be due to solid-state reactions. XRD patterns of the LSF–YSZ composite showed no new phases and no change in the lattice parameter of the perovskite at temperatures below 1473 K [6]. Rather, the decrease in cathode performance is associated with the structural changes shown in Fig. 2. Fig. 2a is an SEM micrograph of the YSZ scaffold prior to the addition of the LSF. The structure is 65% porous, with random, connected openings ranging between 1 and 3 μm in size. After the addition of 40-wt% LSF and calcination to 1123 K, Fig. 2b, a significant fraction of the pore volume is filled with small, well-connected LSF particles, ~0.1 μm in size. Further heating of the LSF–YSZ composite to 1373 K, Fig. 2c, caused the small LSF particles to sinter into a film that uniformly covers the YSZ pores. LSF film formation could reduce electrode performance by decreasing the length of the three-phase boundary (TPB) or by decreasing the LSF surface area available for adsorption. Since the oxygen-ion conductance of LSF is significantly lower than that of YSZ [26], electrode performance may also be limited by transport of O^{2-} in the 1373-K cathode.

The characteristics of LSM cathodes formed by infiltration and calcined at either 1123 or 1373 K are shown in Fig. 3. Fig. 3a provides the *V–i* polarization curves for cells operating at 973 K, while Fig. 3b shows the analogous OCV impedance data. Because the performance of LSM–YSZ electrodes changes after polarization [34–38], data were first obtained after holding the cells at open-circuit overnight and with measurement of the *V–i* curve starting at open-circuit. Then the cells were shorted for 2 h before again measuring the OCV impedance and *V–i* polarization curve. The cell with the 1123-K, LSM–YSZ cathode exhibited a relatively straight *V–i* relationship and was essentially unaffected by polarization. The total ohmic impedance was 0.35 Ω cm^2, again in reasonable agreement with the resistance calculated for the 70-μm YSZ electrolyte, while the total non-ohmic, OCV impedance was 0.7–0.8 Ω cm^2, with ~0.6 Ω cm^2 coming from the cathode. As in the case with LSF, this is slightly higher than the 0.4 Ω cm^2 impedance reported previously for infiltrated LSM calcined to 1123 K [24], which is likely

due to the lower surface area of the YSZ scaffold. The YSZ scaffold in that study was reported to have a greater surface area, 0.76 $m^2\ g^{-1}$ versus 0.26 $m^2\ g^{-1}$; and the performance of infiltrated electrodes has been shown to correlate with scaffold structure [33]. Finally, the impedance of the 1123-K, LSM–YSZ composite decreased by only 0.2 $\Omega\ cm^2$ after 2 h polarization.

The *V–i* relationship for the cell with the 1373-K cathode showed much greater curvature. While the ohmic losses for this cell were similar to that of the cell with the 1123-K cathode, the total OCV impedance was much higher, 2.6 $\Omega\ cm^2$. Another dramatic difference is that the 1373-K, LSM–YSZ electrode exhibited strong hysteretic behavior. After shorting this cell for 2 h, the total non-ohmic, OCV impedance dropped from ~2.3 $\Omega\ cm^2$ to less than 0.7 $\Omega\ cm^2$, a value very close to that obtained for the 1123-K, LSM–YSZ electrode. Furthermore, the *V–i* polarization curve shifted so that it nearly overlapped with that of the cell with the 1123-K cathode. This improved performance was reversible; when the cell with the 1373-K, LSM–YSZ cathode was left at open-circuit overnight, the performance reverted back to that of the unpolarized cell.

Previous XRD data have demonstrated that solid-state reactions between LSM and YSZ are minimal at temperatures below 1373 K [24,39]. Therefore, SEM measurements, shown in Fig. 4, were performed to understand the effect of increased calcination temperature. Similar to what was observed with LSF, LSM formed small, interconnected particles in the pores of the YSZ after calcination at 1123 K, Fig. 4a. After calcination to 1373 K, the LSM formed what appears to be a dense coating over the YSZ pores, Fig. 4b. Given the low ionic conductivity of LSM [40], it is not surprising that a composite in which LSM coats the YSZ pores would have a short TPB and perform poorly. What is less clear is why the coated structure would be affected by polarization and the particle-filled pores would not. While there is still no consensus about what causes the hysteretic behavior in LSM cathodes [2,5], the idea that the morphology of the LSM in the pores would affect this is consistent with a recent report suggesting that hysteresis is associated with movement of the LSM during oxidation and reduction [41].

3.2. Effect of additives on LSF–YSZ cathodes

A variety of additives were incorporated into the LSF–YSZ electrodes and the results are summarized in Figs. 5 and 6 and in Table 1. Fig. 5 shows the *V–i* polarization curves for cells made with LSF–YSZ composites that were first calcined to 1373 K, then infiltrated with the salts needed to incorporate either 0.5-wt% Pd, 10-wt% YSZ, 10-wt% CaO, or 10-wt% K_2O, and finally re-calcined at 973 K. All of the cells showed significant improvement in impedance with the additives. For the cell with 10-wt% K_2O, the slope near OCV was similar to that of the cells with the other additives, but the impedance increased at higher current densities. The effect of additives is seen more clearly by focusing on the *V–i* polarization curves

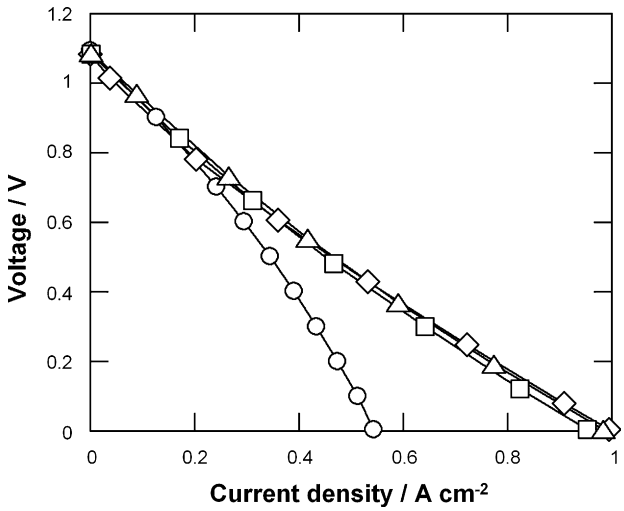

Fig. 5. Performance data for cells with an LSF–YSZ cathode that was calcined to 1373 K after infiltration of either 0.5 wt% Pd (◊), 10 wt% YSZ (△), 10 wt% CaO (□), and 10 wt% K_2O (○).

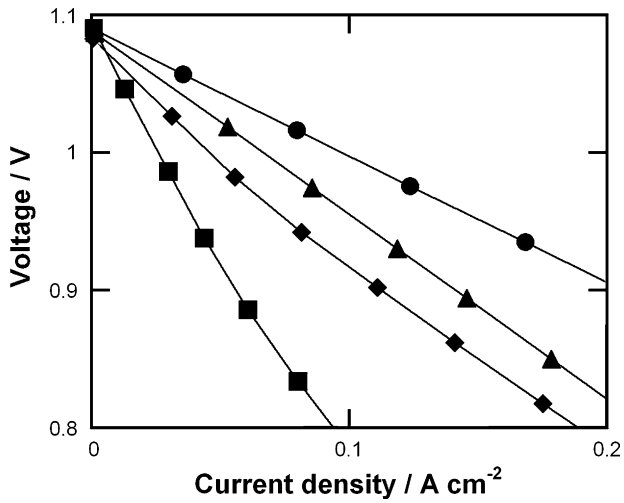

Fig. 6. Performance data for cells with an LSF–YSZ cathode calcined to 1123 K (●), calcined to 1373 K (■), and calcined to 1373 K followed by infiltration of 0.5 wt% Pd (♦) and 10 wt% YSZ (▲).

in the region near OCV, for which selected results are reported in Fig. 6. The dramatic difference between cells with LSF–YSZ cathodes calcined at 1123 and 1373 K is readily apparent in this figure. The addition of 0.5-wt% Pd or 10-wt% YSZ to 1373-K cathodes brings the initial slope closer to that of the 1123-K cathode but 1373-K cathodes with additives still exhibit somewhat poorer performance.

Table 1
Summary of effects of calcination temperatures and infiltrated materials on LSF–YSZ composite cathodes.

LSF calcination temperature (K)	Infiltrated material and wt% added	Second calcination temperature (K)	Non-ohmic impedance at OCV ($\Omega\ cm^2$)
1123	None	None	0.35
1373	None	None	2.60
1123	10-wt% YSZ	973	0.30
1123	10-wt% YSZ	1373	3.30
1373	1.5-wt% YSZ	973	0.75
1373	10-wt% YSZ	973	0.70
1373	0.5-wt% Pd	973	1.25
1373	10-wt% CaO	973	0.70
1373	10-wt% K_2O	973	0.70
1373	10-wt% SDC	973	0.45
1373	0.1N HNO_3	973	2.60
1373	0.1N NH_4OH	973	2.65

Finally, even though the OCV impedances of the 1373-K cathodes were different following the addition of 0.5-wt% Pd (non-ohmic impedance of 1.25 Ω cm^2) and 10-wt% YSZ (non-ohmic impedance of 0.70 Ω cm^2), this had a relatively small effect on the overall *V–i* curves shown in Fig. 5 because the impedances decreased with current density.

Because all of the additives, with the exception of K_2O, affected cell performance in a similar way, the results for the various cells that were tested can be characterized by a single number, the total non-ohmic impedance at OCV. None of the dopants affected the ohmic impedances and only K_2O exhibited the deleterious behavior at higher current densities. In this study, the impedances were measured at 973 K, on similar cells with anodes that had an impedance of approximately 0.15 Ω cm^2, as discussed in the previous section. Table 1 reports the initial calcination temperature of the LSF–YSZ electrodes, the amount and type of dopant, the calcination temperature used after incorporation of the dopant, and the total electrode impedance. For the cell with 0.5 wt% Pd, Table 1 shows a non-ohmic impedance of 1.25 Ω cm^2 near OCV. While this non-ohmic impedance is larger than the values seen for the other infiltrated cells, it still represents a dramatic improvement relative to the 1373-K, LSF–YSZ cell performance, as illustrated in Fig. 6. That the non-ohmic impedance near OCV of the cell with Pd was larger than that of the other infiltrated cells could be due to the significantly lower weight loading of Pd compared to the amounts used with the other additives.

Only one 1123-K LSF–YSZ cell was tested after the addition of a dopant, 10-wt% YSZ in that case. While the non-ohmic impedance on this cell was slightly lower than that of the undoped cell, 0.30 Ω cm^2 versus 0.35 Ω cm^2, the difference was so small that the significance of this improvement was unclear. A more interesting result was that obtained after the addition of 10-wt% YSZ onto the 1123-K composite, followed by calcination to 1373 K. It was expected that the YSZ would partially fill in the space between the LSF particles and modify film formation. Unfortunately, the non-ohmic impedance of this cell was similar to that of the undoped, 1373-K LSF–YSZ composite.

The data in Table 1 also highlight several other important observations. First, the greatest improvement in performance in our studies was achieved by adding 10-wt% $Ce_{0.8}Sm_{0.2}O_{1.9}$ (SDC). The non-ohmic impedance for that cell was only 0.45 Ω cm^2. Whether this is significant compared to the improvement with the addition of 10-wt% YSZ is uncertain. Second, only small quantities of dopant are required to enhance performance. The non-ohmic losses decreased to 0.75 Ω cm^2 after the addition of only 1.5-wt% YSZ. Finally, the enhanced performance achieved by infiltration of various compounds into the 1373-K LSF–YSZ electrode is probably not associated with the infiltration process itself. If the liquid used in the infiltration step were simply restructuring the LSF film, the infiltration of either a weak acid or weak base, 0.1N HNO_3 and 0.1N NH_4OH, should have modified the performance in a similar manner as that observed with the dopants. However, the infiltration of HNO_3 and NH_4OH, both of which will be completely removed following calcination at 973 K, had no effect on performance.

3.3. Characterization of LSF–YSZ cathodes

XRD measurements were taken of LSF–YSZ cathodes calcined to 1123 and 1373 K and of 1373 K calcined samples infiltrated with the promoters used in this study. The XRD data obtained for the low and high-temperature calcined samples were in agreement with results obtained in previous studies, showing most importantly that no phases were present other than those of the YSZ and the perovskite. With higher temperature calcination, the perovskite peaks narrowed which is consistent with the sintering of LSF into larger crystallites. None of the infiltrated species were observed in the XRD spectra, apparently due to the low weight loadings and broad diffraction lines. Since all of the dopants improved the performance of the 1373-K, LSF–YSZ composite, we examined several of the composites by SEM and Brunauer–Emmett–Teller (BET) isotherms to determine what changes occurred in the electrode microstructure following dopant incorporation. As reported in a previous work, the surface area of the LSF–YSZ cathode is highly dependent on calcination temperature. As shown in Table 2, the infiltration of LSF into the YSZ scaffold shows a significant increase in surface area when calcined to 1123 K, but this increased surface area is lost when the electrode is calcined further to 1373 K. When additional materials are infiltrated into the 1373-K, LSF–YSZ, there are again increases in surface area, although not to the levels measured in the 1123-K, LSF–YSZ cell, accept for when 10-wt% YSZ was added.

Table 2
Surface areas measured from BET isotherms using Kr at 78 K.

Sample	Surface area (m^2 g^{-1})
YSZ scaffold	0.26
LSF–YSZ calcined at 1123 K	1.80
LSF–YSZ calcined at 1373 K	0.30
LSF–YSZ (1373 K) with 0.5 wt% Pd (973 K)	0.46
LSF–YSZ (1373 K) with 10 wt% CaO (973 K)	0.62
LSF–YSZ (137 3K) with 10 wt% K_2O (973 K)	0.60
LSF–YSZ (1373 K) with 10 wt% YSZ (973 K)	2.56
LSF–YSZ (1373 K) with 10 wt% YSZ (1373 K)	0.40

Micrographs of composites with 0.5-wt% Pd, 10-wt% YSZ, and 10-wt% CaO are shown in Fig. 7. Fig. 7a, the micrograph with 0.5-wt% Pd, suggests that the LSF film is relatively unaffected. The Pd is present as small, 0.1-μm particles on top of the LSF film. This is consistent with the tendency of metals to interact weakly with oxides and the relatively large size of the Pd particles is simply due to the very low surface area of the LSF–YSZ composite. The micrograph in Fig. 7b shows that the composite with added YSZ has a very different appearance. In this case, the LSF film is covered by a rough film of the YSZ. Finally, the CaO deposits, shown in Fig. 7c, appear as angular-shaped crystals over the LSF. Although the results are not reported here, structures similar to those observed in the YSZ and CaO infiltrated cells were seen in the cells infiltrated with SDC and K_2O, respectively. While these SEM images may not be depicting features at TPB sites, the micrographs in Fig. 6 reveal no obvious commonalities between Pd, YSZ (SDE), and CaO.

3.4. Effect of additives on LSM–YSZ cathodes

In our studies of promotion in LSM–YSZ composites, we focused on improving the electrodes calcined to 1373 K. The effect of each promoter can again be described by the OCV impedance, measured before and after polarizing the cell, and is summarized in Table 3. As discussed earlier, the cell with the 1123-K, LSM–YSZ electrode exhibited a relatively low non-ohmic impedance of 0.8 Ω cm^2 at 973 K and this decreased to 0.6 Ω cm^2 after shorting the cell for 2 h. The cell with the 1373-K, LSM–YSZ electrode had a non-ohmic impedance of 2.3 Ω cm^2 prior to polarization but showed a similar impedance, 0.7 Ω cm^2, to that of the low-temperature composite after shorting.

The addition of 10-wt% CeO_2 or 1-wt% Pd to the 1373-K composite decreased the OCV impedances dramatically. The total non-ohmic losses in the cell with 10-wt% CeO_2 decreased to 0.5 Ω cm^2, which is only slightly higher than that of the cells with LSF-based electrodes, while the cell with 0.5-wt% Pd decreased to 0.8 Ω cm^2. Both cells were also affected much less by polarization. The addition of 10-wt% YSZ also decreased the non-ohmic impedance, but only to 1.3 Ω cm^2, and this cell was affected more strongly by polarization.

Table 3
Summary of effects of calcination temperatures and infiltrated materials on LSM–YSZ composite cathodes.

LSM calcination temperature (K)	Infiltrated material and wt% added	Second calcination temperature (K)	Non-ohmic impedance at OCV ($\Omega\,cm^2$)	Non-ohmic impedance at OCV after polarization ($\Omega\,cm^2$)
1123	None	None	0.80	0.60
1373	None	None	2.30	0.70
1373	10-wt% CeO_2	973	0.50	0.50
1373	10-wt% CeO_2	1373	2.50	1.35
1373	10-wt% YSZ	973	1.30	0.70
1373	0.5-wt% Pd	973	0.80	0.55
1373	0.1 M NH_4NO_3	973	1.90	1.20

Unfortunately, calcination of an electrode with 10-wt% CeO_2 to 1373 K caused the impedance to increase to a value higher than the unpromoted case. The non-ohmic impedance of this cell increased to 2.5 $\Omega\,cm^2$ and shorting for 2 h reduced this to only 1.3 $\Omega\,cm^2$. In a study of the stability of LSF–YSZ electrodes formed by infiltration [6], it was argued that operation of an electrode for several thousand hours is equivalent to calcination for shorter times at 1373 K. If this is true for the ceria-doped LSM–YSZ electrodes, the improvement associated with the addition of ceria will not give stable performance. A similar point was made by Mogensen et al., for conventional LSM–YSZ electrodes promoted by ceria [20].

4. Discussion

Several important observations can be taken from the data in this paper. First, even without the addition of promoters, LSF–YSZ and LSM–YSZ electrodes formed by infiltration exhibited a number of common features. For both cases, electrodes formed after low-temperature (1123 K) calcination were composed of fine perovskite particles within the YSZ pore structure. These electrodes exhibited low impedances that are nearly independent of current density. After high-temperature (1373 K) calcination, both LSM and LSF formed films that appear to coat the YSZ pores. The impedances on the 1373-K electrodes were much larger at

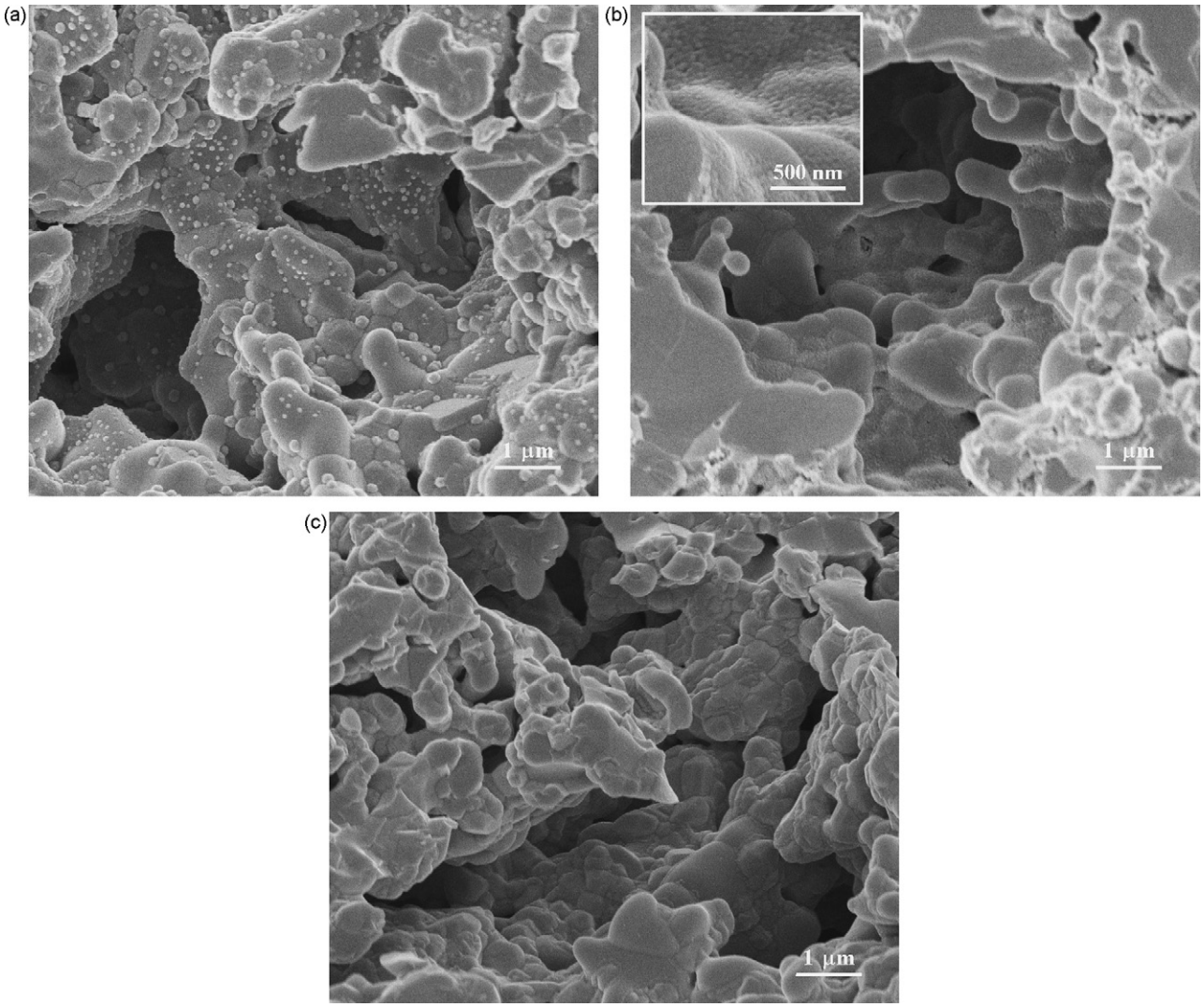

Fig. 7. (a) An SEM image of the LSF–YSZ composite prepared by calcination at 1373 K with 0.5-wt% Pd. (b) An SEM image of the LSF–YSZ composite prepared by calcination at 1373 K with 10-wt% YSZ. (c) An SEM image of the LSF–YSZ composite prepared by calcination at 1373 K with 10-wt% CaO.

open-circuit but decreased significantly with current density. The major difference between the LSM and LSF electrodes was that the high-temperature LSM exhibited hysteretic behavior, with the impedance decreasing dramatically after application of a current. Interestingly, the performance of the 1373-K LSM–YSZ electrode after activation was similar to that of the 1123-K composite. Since the conventional preparation of composite cathodes involves calcination at temperatures above 1273 K, it is possible that the relatively poor performance of LSF-based cathodes compared to ones based on LSM is due to the ability of LSM to improve under a load.

A recent study has argued that the non-stationary behavior of LSM-based electrodes is associated with formation of an LSM film under oxidizing conditions that can then break up under the reducing conditions imposed near TPB sites by a cathodic overpotential [41]. That picture is consistent with the morphological changes observed by SEM in the present study. Unfortunately, it was not simple to observe the formation of nano-pores following electrode polarization by SEM, since these would only be expected to form in the vicinity of the electrolyte interface, where the reducing conditions caused by polarization would be most severe. Still, circumstantial evidence – the fact that the 1123-K electrode shows performance characteristics similar to that of the electrode calcined at 1373 K after activation – points towards the importance of LSM morphology in determining properties. The relatively low calcination temperatures used in the present study for even the "high-temperature" composites makes it less likely that formation of interfacial compounds is responsible for the observed behavior.

The bigger question concerns what the promoters are doing to enhance performance. The fact that Pd, CeO_2 (or SDC), YSZ, CaO, and K_2O are all capable of decreasing the electrode impedance of LSM and LSF cathodes argues that the effect is not primarily to enhance either catalytic or ionic conductivities. For example, if promotion were due to catalytic effects, Pd and CaO should have given dramatically different enhancements. The fact that the addition of each promoter to the 1373-K LSM and LSF electrodes caused the electrodes to exhibit a performance that approaches that of their 1123-K counterparts suggests that the addition of the promoters is somehow related to structure and possibly to the surface area of the cathode. Indeed, the only obvious correlation observed in the present study was between performance and electrode surface area. The fact that recalcination of the promoted electrodes to 1373 K caused them to revert back to their initial state is further evidence that enhanced performance is related to structure. Exactly how each of the modifiers affects the structure near the TPB sites is unclear at this point.

An important lesson to be taken from this study is that one should be careful in interpreting the results of studies in which a single modifier, or even a single class of modifiers is used, since a simple explanation for the observed results may not be applicable. If only species that were expected to be catalytic had been added, we would have concluded that the dopants had enhanced performance by increasing the oxidation rates of the cathode. Based on the fact that similar enhancements were obtained for Pd and CaO, it seems unlikely that catalytic effects are responsible for our observations. An additional complication is that the influence of additives appears to depend on the initial electrode structure [21,22]. This helps to explain some of the discrepancies in literature over whether certain dopants enhance performance or not.

Finally, one very clear conclusion from this study is that our fundamental understanding of electrode processes in SOFC is insufficient. Despite the large body of work on SOFC cathodes [2], the main factors that limit performance are still uncertain.

5. Conclusion

The major conclusion of the present study is that electrode promotion through the addition of catalytic and conducting components is associated with electrode structure, at least for the systems studied here. None of the additives studied had any effect on electrode performance for composites calcined at 1123 K, while enhanced electrode performance was observed with almost all of the additives, for both LSF–YSZ and LSM–YSZ electrodes, if the composites had first been calcined to 1373 K. Dopants that were not expected to enhance either catalytic or ionic-conductivity properties were equally effective to dopants that were. That enhancement is related to electrode structure helps to explain disagreements in the literature over whether certain additives decrease electrode overpotentials.

Acknowledgements

This work was funded by the U.S. Department of Energy's Hydrogen Fuel Initiative (Grant DE-FG02-05ER15721). G. Kim acknowledges support from the WCU (World Class University) program through the Korea Science and Engineering Foundation, which is funded by the Ministry of Education, Science and Technology (R31-2008-000-20012-0).

References

[1] F. Tietz, Q. Fu, V.A.C. Haanappel, A. Mai, N.H. Menzler, S. Uhlenbruck, Int. J. Appl. Ceram. Technol. 4 (2007) 436.
[2] S.B. Adler, Chem. Rev. 104 (2004) 4791.
[3] J. Fleig, J. Maier, J. Eur. Ceram. Soc. 24 (2004) 1343.
[4] N.Q. Minh, J. Am. Ceram. Soc. 76 (1993) 563.
[5] J.M. Vohs, R.J. Gorte, Adv. Mater. 21 (2009) 943.
[6] W. Wang, M.D. Gross, J.M. Vohs, R.J. Gorte, J. Electrochem. Soc. 154 (2007) B439.
[7] H. Uchida, M. Yoshida, M. Watanabe, J. Electrochem. Soc. 146 (1999) 1.
[8] J.W. Erning, T. Hauber, U. Stimming, K. Wipperman, J. Power Sources 61 (1996) 205.
[9] V.A. Haanappel, D. Rutenbeck, A. Mai, S. Uhlenbruck, D. Sebold, H. Wesemeyer, B. Rowekamp, C. Tropartz, F. Tietz, J. Power Sources 130 (2004) 119.
[10] K. Yamahara, C.P. Jacobson, S.J. Visco, L.C. de Jonghe, Solid State Ionics 176 (2005) 451.
[11] K. Yamahara, C.P. Jacobson, S.J. Visco, X.F. Zhang, L.C. de Jonghe, Solid State Ionics 176 (2005) 275.
[12] Y. Huang, J.M. Vohs, R.J. Gorte, J. Electrochem. Soc. 153 (2006) A951.
[13] R. Chiba, F. Yoshimura, Y. Sakurai, Y. Tabata, M. Arakawa, Solid State Ionics 175 (2004) 23.
[14] C. Lu, T.Z. Sholklapper, C.P. Jacobson, S.J. Visco, L.C. De Jonghe, J. Electrochem. Soc. 153 (2006) A1115.
[15] C.C. Kan, E.D. Wachsman, J. Electrochem. Soc. 156 (2009) B695.
[16] S.P. Jiang, W. Wang, J. Electrochem. Soc. 152 (2005) A1398.
[17] Z. Jiang, L. Zhang, K. Feng, C. Xia, J. Power Sources 185 (2008) 40.
[18] Y.-K. Lee, J.-Y. Kim, Y.-K. Lee, I. Kim, H.-S. Moon, J.-W. Park, C.P. Jacobson, S.J. Visco, J. Power Sources 115 (2003) 219.
[19] S.P. Simner, M.D. Anderson, M.H. Engelhard, J.W. Stevenson, Electrochem. Solid-State Lett. 9 (2006) A478.
[20] M. Mogensen, M. Søgaard, P. Blennow, K.K. Hansen, 8th European SOFC Forum Lucerne, Switzerland, Lucerne Fuel Cell Forum, 2008, paper A0402.
[21] S.P. Jiang, Y. Ye, T. He, S.B. Ho, J. Power Sources 185 (2008) 179.
[22] G. Kim, S. Lee, J.Y. Shin, G. Corre, J.T.S. Irvine, J.M. Vohs, R.J. Gorte, Electrochem. Solid-State Lett. 12 (2009) B48.
[23] G. Kim, G. Corre, J.T.S. Irvine, J.M. Vohs, R.J. Gorte, Electrochem. Solid-State Lett. 11 (2008) B16.
[24] Y. Huang, J.M. Vohs, R.J. Gorte, J. Electrochem. Soc. 152 (2005) A1347.
[25] A. Trovarelli, Catal. Rev. Sci. Eng. 38 (1996) 439.
[26] F. Bidrawn, S. Lee, J.M. Vohs, R.J. Gorte, J. Electrochem. Soc. 155 (2008) B660.
[27] S. Park, R.J. Gorte, J.M. Vohs, J. Electrochem. Soc. 148 (2001) A443.
[28] R.J. Gorte, S. Park, J.M. Vohs, C. Wang, Adv. Mater. 12 (2000) 1465.
[29] Y. Huang, J.M. Vohs, R.J. Gorte, J. Electrochem. Soc. 151 (2004) A646.
[30] Y. Huang, J.M. Vohs, R.J. Gorte, Electrochem. Solid-State Lett. 9 (2006) A237.
[31] G. Kim, J.M. Vohs, R.J. Gorte, J. Mater. Chem. 18 (2008) 2386.
[32] K. Sasaki, J. Maier, Solid State Ionics 134 (2000) 303.
[33] Y. Huang, K. Ahn, J.M. Vohs, R.J. Gorte, J. Electrochem. Soc. 151 (2004) A1592.
[34] S. McIntosh, S.B. Adler, J.M. Vohs, R.J. Gorte, Electrochem. Solid-State Lett. 7 (2004) A111.
[35] S.P. Jiang, J.G. Love, Solid State Ionics 138 (2001) 183.

[36] M.J. Jorgensen, S. Primdahl, M. Morgensen, Electrochim. Acta 44 (1999) 4195.
[37] F.H. van Heuveln, H.J.M. Bouwmeester, J. Electrochem. Soc. 144 (1997) 134.
[38] S.P. Jiang, J. Mater. Sci. 43 (2008) 6799.
[39] H. Yokokawa, H. Tu, B. Iwanschitz, A. Mai, J. Power Sources 182 (2008) 400.
[40] Y. Ji, J.A. Kilner, M.F. Carolan, Solid State Ionics 176 (2005) 937.
[41] L.Y. Woo, R.S. Glass, R.J. Gorte, C.A. Orme, A.J. Nelson, J. Electrochem. Soc. 156 (2009) B602.